ISSN 1063-7761, Journal of Experimental and Theoretical Physics, 2012, Vol. 114, No. 6, pp. 955–962. © Pleiades Publishing, Inc., 2012.
Original Russian Text © V.I. Zinenko, N.G. Zamkova, V.S. Zhandun, M.S. Pavlovskii, 2012, published in Zhurnal Eksperimental'noi i Teoreticheskoi Fiziki, 2012, Vol. 141, No. 6, pp. 1093–1101.

SOLIDS AND LIQUIDS

Ferroelectric and Structural Instability in Double Perovskites $Me^{1+}Bi^{3+}Me^{3+}Nb^{5+}O_6$ (Me^{1+} = Na, K, Rb; Me^{3+} = Sc, Ga, In, Lu)

V. I. Zinenko, N. G. Zamkova, V. S. Zhandun, and M. S. Pavlovskii

Kirenskii Institute of Physics, Siberian Branch, Russian Academy of Sciences, Akademgorodok, Krasnoyarsk, 660036 Russia
e-mail: zvi@iph.krasn.ru

Received July 27, 2011

Abstract—Within the Gordon–Kim generalized model with regard to the polarizabilities of ions, the lattice constants, the high-frequency permittivity, the Born dynamic charges, and the vibration constants of the crystal lattice are calculated for cation-ordered double perovskites $Me^{1+}Bi^{3+}Me^{3+}Nb^{5+}O_6$. The vibration spectra of all the compounds exhibit two types of instabilities: instability associated with the rotation of the oxygen octahedron and ferroelectric instability. Various combinations of distortions with respect to the rotation mode yield five energetically most favorable distorted phases. The symmetry and the energy characteristics of these phases are discussed. In four of the five phases, the distortions associated with the oxygen octahedron rotation lead to polar phases, thus allowing one to speak of improper ferroelectricity in these compounds. One phase turns out to be nonpolar; however, it contains unstable polar modes such that a displacement along the eigenvectors of these modes gives rise to polarization in the crystal.

DOI: 10.1134/S1063776112040188

1. INTRODUCTION

ABO_3 ferroelectrics with perovskite structure have been studied for a few decades. In recent years, complex compounds synthesized on the basis of ABO_3 oxides have been the subject of especially intense research. The ferroelectric properties of these compounds substantially depend on their chemical composition, and, together with simple perovskite oxides, these compounds find application in the technology of electronic devices such as ferroelectric memory, piezoelectric sensors, piroelectric devices, etc.

On the other hand, the study of these compounds is also interesting from the fundamental point of view, providing an insight into the microscopic sources of their diverse, and sometimes unique, physical properties. As a rule, in both simple and complex perovskite-like oxides, irrespective of whether or not they are cation-ordered, there are two types of lattice instability in a high-symmetry (cubic or tetragonal) phase: ferroelectric instability and the so-called antiferrodistorsive instability associated with the rotation of the BO_6 octahedron.

The ferroelectric instability depends on a fine balance between long-range dipole–dipole and short-range interactions. Owing to the high polarizability of oxygen ions and a specific feature of the perovskite structure, large dipole–dipole attraction interactions contribute to polar distortions of the structure, whereas the short-range repulsion interactions stabilize the high-symmetry phase.

The antiferrodistorsive instability also depends on the balance between short-range repulsion forces, which, on the contrary, contribute to distortions due to the rotation of the octahedron, and long-range Coulomb interactions between point charges, which hamper the development of these distortions. Long-range dipole–dipole interactions do not play any significant role in the antiferrodistorsive instability. A large number of publications have been devoted to the discussion of these two types of instabilities in simple and complex oxides with perovskite structure (see the recent surveys [1] and references therein).

Both ferroelectric and antiferrodistorsive instabilities substantially depend on the chemical composition of compounds and the degree of cation ordering in complex oxides. Thus, the study of the dynamics of a crystal lattice and finding out details of the above-mentioned balance between long-range and short-range interactions in both known and as yet not synthesized compounds is of topical interest.

In the present paper, we consider virtually unstudied compounds $Me^{1+}Bi^{3+}Me^{3+}Nb^{5+}O_6$ (Me^{1+} = Na, K, Rb; Me^{3+} = Sc, Ga, In, Lu). In [2], the authors reported on the synthesis of the compound $NaBiScNbO_6$ and gave tentative information on its structure with the space group *Pnma* and with the unit-cell parameters $a = b = 5.631$ Å and $c = 7.963$ Å. We could not find any information on the study of the physical properties of this compound and on the synthesis of other compounds of the above-mentioned series in the literature. In [3], the authors analyzed the effect of Me^{1+} (Me^{1+} = Na, K, Rb) ion in $Me^{1+}BiScNbO_6$ on the polar behavior of these com-

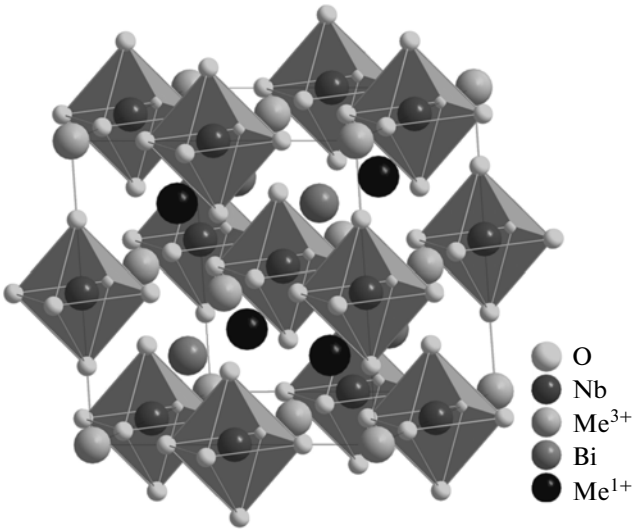

Fig. 1. Structure of the cubic phase of the cation-ordered compound $Me^{1+}BiMe^{3+}NbO_6$.

pounds by the density functional method with the use of QUANTUM ESPRESSO software package. The authors of [3] considered a 40-atom cell with ordering with respect to both NaCl-type cations, relaxed the structure, and calculated the angles of rotation of the NbO_6 octahedron and the spontaneous polarization and the Born effective charges in the relaxed structure. However, they did not calculate the lattice dynamics.

The aim of the present study is a nonempirical calculation of the equilibrium lattice parameters, the high-frequency permittivity, the Born effective charges, and the lattice dynamics of the compounds $Me^{1+}BiMe^{3+}NbO_6$ (Me^{1+} = Na, K, Rb; Me^{3+} = Sc, Ga, In, Lu) in a cubic perovskite structure ordered with respect to the cations (Me^{1+}, Bi) and (Me^{3+}, Nb) in the [111] direction; the analysis of the structure and energy characteristics of phases with polar and antiferrodistortive distortions; and the calculation of spontaneous polarization in the distorted phases.

2. METHOD OF CALCULATION

The calculations have been carried out by the density functional method within the Gordon–Kim ionic crystal model with polarizable ions. The details of the model are described in [4]. The unit-cell parameters, elasticity constants, dielectric constants, the Born effective charges, and the spectrum of lattice vibration frequencies have been calculated for a face-centered cubic lattice with the space group $F\text{-}43m(T2d)$ with one molecule of $Me^{1+}BiMe^{3+}NbO_6$ in the unit cell, as is shown in Fig. 1. Here the ions occupy the following positions:

$$Me^{1+}\left(\frac{1}{2}, \frac{1}{2}, \frac{1}{2}\right), \quad Bi\left(\frac{3}{2}, \frac{3}{3}, \frac{3}{2}\right),$$

$$Me^{3+}(0, 0, 0), Nb(1, 1, 1), O\left(\frac{1}{2}, \frac{1}{2}, z\right).$$

The lattice dynamics, the rotation angles of the NbO_6 octahedron, and the spontaneous polarization in distorted phases have been calculated for a 40-atom simple cubic lattice with doubled unit-cell parameter of the perovskite lattice.

The displacements of ions from their positions in the cubic phase have been calculated as follows: at the first step, we calculated the displacements of ions along the eigenvectors of the rotation modes of vibrations and determined the corresponding angles by minimizing the total energy with respect to the amplitude of these displacements. Then we relaxed the structure by an iterative method. To this end, we calculated the forces

$$f_j^\alpha = \frac{\partial E^{\text{tot}}}{\partial r_i^\alpha},$$

for each ion; here E^{tot} is the total energy of the crystal, which represents the following sum of contributions: $E^{\text{tot}} = E^{\text{coul}} + E^{\text{short}} + E^{\text{dip}}$. Note that, in this model, all the contributions to the total energy of the crystal have analytic expressions (see survey [4]); therefore, the first derivative of energy is calculated analytically, rather than numerically, from the expression for the total energy given in [4]. Next, each ion was displaced in the direction of the force acting on this ion. Then we again calculated the forces acting on the ions and repeated the procedure until the forces on each ion do not exceed $\delta = 2$ meV/A. After the relaxation, we calculated the limiting vibration frequencies of the relaxed 40-atom crystal lattice. When the vibration spectrum of the relaxed structure contained imaginary frequencies, we distorted the structure along the eigenvectors of these unstable polar modes and again applied the relaxation procedure.

3. RESULTS AND DISCUSSION

3.1. Dynamics of a Crystal Lattice

Table 1 presents the calculated values of the unit-cell parameters, elasticity moduli, and high-frequency permittivity for all the compounds in the cubic phase. This table also presents the lattice parameter of the $NaBiScNbO_6$ crystal recalculated from the experimental data for the rhombic phase [2]. (Note that, according to the space group and the values of the lattice parameters, the authors of [2] considered a compound totally disordered with respect to the cations of Na, Bi and Sc, Nb.) We can see that the calculated

Table 1. Unit-cell parameters, free coordinate of oxygen, elasticity moduli, and high-frequency permittivity of the compounds $Me^{+1}BiMe^{+3}NbO_6$ in the cubic phase

	a, Å	O: [1/2; 1/2; z]	C_{11}, GPa	C_{12}, GPa	C_{44}, GPa	ε_∞
$NaBiScNbO_6$	7.83	0.74	249.22	82.25	80.14	6.65
$NaBiGaNbO_6$	7.89	0.74	244.37	78.64	76.82	5.43
$NaBiInNbO_6$	8.05	0.735	244.00	68.78	66.51	5.34
$NaBiLuNbO_6$	8.13	0.735	245.24	64.47	62.23	4.26
$KBiScNbO_6$	7.87	0.74	244.47	84.63	82.67	6.54
$KBiGaNbO_6$	7.92	0.74	241.15	81.23	79.36	5.49
$KBiInNbO_6$	8.08	0.735	239.95	70.88	68.80	5.33
$KBiLuNbO_6$	8.16	0.735	240.69	66.35	64.41	4.33
$RbBiScNbO_6$	7.91	0.74	238.38	86.11	84.32	6.52
$RbBiGaNbO_6$	7.96	0.74	234.88	82.63	81.01	5.57
$RbBiInNbO_6$	8.11	0.735	233.24	72.03	70.37	5.33
$RbBiLuNbO_6$	8.19	0.735	235.33	67.69	65.99	4.43

unit-cell parameter is less than the appropriate experimental value by 1.5%. As expected, the unit-cell parameter increases as the radii of the Me^{1+} and Me^{3+} ions increase. At the same time, Table 1 shows that the dielectric constant remains almost unchanged under the substitution Na ⟶ K ⟶ Rb and is significantly changed under the substitution Sc⟶ Ga⟶ In ⟶ Lu. Figure 2 shows the vibration spectrum of the crystal lattice for $NaBiScNbO_6$ (the spectra for the other compounds differ little from this spectrum and are therefore omitted). We can see that the vibration spectrum has two types of unstable modes at the center of the Brillouin zone: the most unstable threefold degenerate nonpolar mode and the less unstable threefold degenerate polar mode. (Figure 2 shows a phonon spectrum with regard to the macroscopic field in LO vibrations.) We can also see that the nonpolar unstable mode occupies the whole volume of the phase space, while the polar mode is unstable in the larger part of this space.

The decomposition of the mechanical representation of these compounds in terms of irreducible representations of the center of the Brillouin zone of the face-centered cubic lattice has the form

$$T = A_1 + E + 2F_1 + 7F_2.$$

The most unstable vibration modes of the lattice at the center and the boundary point X of the Brillouin zone for the cubic phase of all the compounds are presented in Table 2. The eigenvectors of these modes are shown in Fig. 3.

The eigenvectors of the threefold degenerate mode F_1 $(q = 0)$ and of the single mode $X_2\left(q = \frac{2\pi}{a}(1, 0, 0)\right)$ correspond to the antiferrodistortive distortion of the structure. However, the eigenvectors of these modes differ from those in the case of simple perovskites (in this case, the modes F_1 and X_2 correspond to the modes R_{25} at the boundary point $R\left(q = \frac{\pi}{2}(1, 1, 1)\right)$

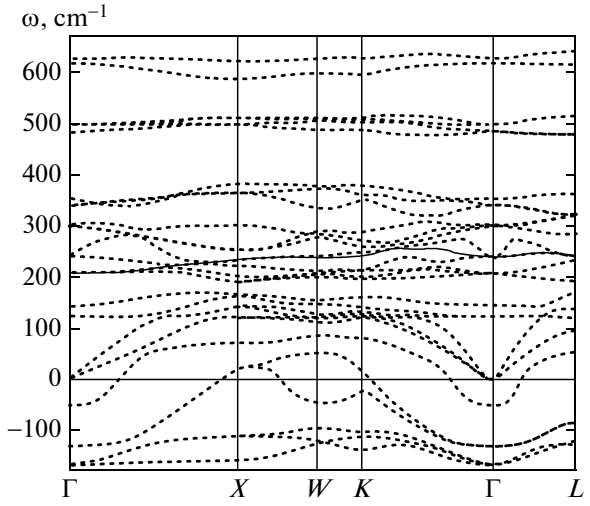

Fig. 2. Phonon spectrum of the compound $NaBiScNbO_6$. Imaginary frequencies are indicated by negative values.

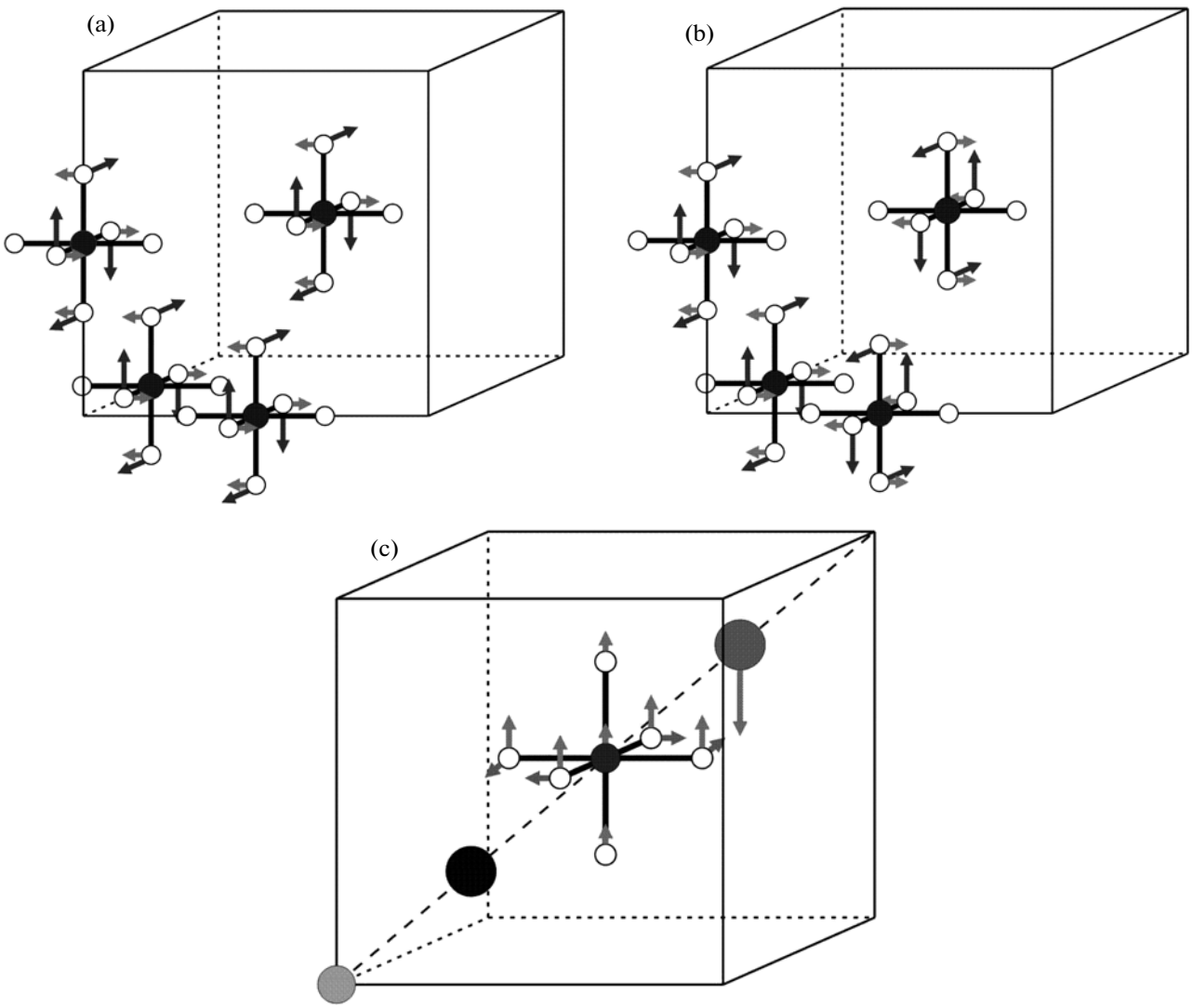

Fig. 3. Displacements of ions along the eigenvectors of unstable modes: (a) one component of the threefold degenerate mode F_1 (φ00 distortion); (b) the mode X_2 (ψ00 distortion); and (c) one component of the threefold degenerate mode F_2 (00*p* distortion). The relative displacements of ions are represented by the arrow length. For a polar mode, the displacements of the Me^{1+} and Me^{3+} ions are not shown because of their negligible value.

and M_3 at the boundary point $M\left(q = \frac{\pi}{a}(1, 1, 0)\right)$ of the perovskite structure) and double perovskites Me_2ABO_6 with the structure of elpasolite (in this case, the modes F_1 and X_2 correspond to the modes Γ_{1g} $(q = 0)$ and $X_3\left(q = \frac{2\pi}{a}(1, 0, 0)\right)$. In addition to the displacements of the oxygen ions, corresponding to the pure rotation of the octahedra NbO_6 and $Me^{3+}O_6$, the eigenvectors of the modes F_1 and X_2 contain the displacements of the same oxygen ions, corresponding to the bending of the Nb–O–Me^{3+} bonds (the amplitude of bending displacements is about half the amplitude of the displacements corresponding to the rotation of the oxygen octahedron), as illustrated in Figs. 3a and 3b. Below, we will denote the distortion related to the modes F_1 $(q = 0)$ and $X_2\left(q = \frac{2\pi}{a}(1, 0, 0)\right)$, $Y_2\left(q = \frac{2\pi}{a}(0, 1, 0)\right)$, $Z_2\left(q = \frac{2\pi}{a}(0, 0, 1)\right)$ by φ and ψ, respectively.

The threefold degenerate unstable mode F_2 $(q = 0)$ is polar; one component of its eigenvector is shown in Fig. 3c. This figure also exhibits a significant difference from the perovskite and elpasolite structures. In addition to the pure displacements of ions along one Cartesian coordinate, there are displacements of a part of oxygen ions in a plane perpendicular to this direction, which correspond to the collapse of the

Table 2. Imaginary vibration frequencies (cm^{-1}) of the compounds $Me^{+1}BiMe^{+3}NbO_6$ in the cubic phase at the center and at a boundary point of the Brillouin zone

	Γ ($q = 0$)		X ($q = 2\pi/a(1; 0; 0)$)
	FE (F_2)	AFD (F_1)	AFD
$NaBiScNbO_6$	132*i*	188*i*	183*i*
$NaBiGaNbO_6$	127*i*	192*i*	186*i*
$NaBiInNbO_6$	134*i*	215*i*	209*i*
$NaBiLuNbO_6$	133*i*	221*i*	215*i*
$KBiScNbO_6$	134*i*	182*i*	174*i*
$KBiGaNbO_6$	128*i*	186*i*	178*i*
$KBiInNbO_6$	134*i*	210*i*	202*i*
$KBiLuNbO_6$	133*i*	216*i*	208*i*
$RbBiScNbO_6$	136*i*	177*i*	168*i*
$RbBiGaNbO_6$	129*i*	182*i*	171*i*
$RbBiInNbO_6$	134*i*	206*i*	196*i*
$RbBiLuNbO_6$	132*i*	213*i*	202*i*

NbO_6 octahedron. Note that, in the unstable polar mode F_2, the Bi^{3+} ions and a part of oxygen ions undergo the largest displacements, as is illustrated in Fig. 3c. Henceforth, we will indicate polar distortions by *p*.

Table 3 presents the Born dynamic charges for all the compounds considered. One can see that the dynamic charges of the bismuth ion and the component $O_\perp$ of the charge of oxygen perpendicular to the Nb–O–Me^{3+} bond are insensitive to the variations of both the alkali metal ion and the trivalent ion in the $Me^{3+}O_6$ octahedron. At the same time, the dynamic charge of the Me^{3+} ion itself and, accordingly, the component $O_\parallel$ of the dynamic charge of oxygen that is parallel to the Nb–O–Me^{3+} bond significantly decrease as the number of the trivalent ion in the periodic table increases. The physics behind this sharp variation in the dynamic charges of Me^{3+} and $O_\parallel$ may be as follows. In the model of ionic crystals with polarizable ions that is used in this study, the high-frequency permittivity and the Born dynamic charges are represented as [5]

$$\varepsilon_\infty = 1 + \frac{4\pi}{\Omega}\alpha_{\text{eff}}\left(1 - \frac{4\pi}{3\Omega}\alpha_{\text{eff}}\right)^{-1},$$

$$Z_{\text{din}}(i) = \frac{\varepsilon_\infty + 2}{3} Z_{\text{eff}}(i),$$

where $Z_{\text{eff}}^{\alpha\beta}(i)$ and $\alpha_{\text{eff}}^{\alpha\beta}$ are, respectively, the effective charge and the polarizability of an ion in the crystal:

$$\alpha_{\text{eff},\,ij}^{\alpha\beta} = \alpha_j[\delta_{\alpha\beta} + \alpha_i(\gamma_{ij}^{\alpha\beta} + \Gamma_{ij}^{\alpha\beta})]^{-1},$$

$$Z_{\text{eff}}^{\alpha\beta}(i) = Z_{\text{ion}}(i)\delta_{\alpha\beta}$$

$$- \sum_{j,\gamma} \alpha_{\text{eff},\,ij}^{\alpha\gamma}\left(T_{ji}^{\gamma\beta} - \left(\frac{4\pi}{3\Omega}\delta_{\gamma\beta} - \gamma_{ji}^{\gamma\beta}\right)Z_{\text{ion}}(j)\right).$$

Here $\gamma_{ij}^{\alpha\beta}$ characterizes the difference between the internal field of the ion and the Lorentz field, and the matrices $\hat{\Gamma}$ and $\hat{T}$ describe short-range interactions between large dipoles and between large dipoles and spherically distributed charge of the ion, respectively.

Table 3. Born dynamic charges (in the units of electron charge) of the compounds $Me^{+1}BiMe^{+3}NbO_6$ in the cubic phase

	Z_{din}^{A}	$Z_{\text{din}}^{A'}$	Z_{din}^{B}	$Z_{\text{din}}^{B'}$	$Z_{\text{din}}^{O_\parallel}$	$Z_{\text{din}}^{O_\perp}$
$NaBiScNbO_6$	1.20	4.32	5.66	6.95	−6.23	−1.42
$NaBiGaNbO_6$	1.18	4.15	3.01	5.93	−3.99	−1.57
$NaBiInNbO_6$	1.21	4.19	2.66	6.41	−3.83	−1.70
$NaBiLuNbO_6$	1.19	4.01	1.37	5.35	−2.32	−1.82
$KBiScNbO_6$	1.36	4.38	5.56	6.87	−6.15	−1.46
$KBiGaNbO_6$	1.30	4.22	3.12	5.95	−4.08	−1.61
$KBiInNbO_6$	1.33	4.24	2.82	6.37	−3.90	−1.74
$KBiLuNbO_6$	1.27	4.07	1.57	5.38	−2.43	−1.86
$RbBiScNbO_6$	1.28	4.46	5.48	6.78	−6.11	−1.44
$RbBiGaNbO_6$	1.22	4.31	3.23	5.95	−4.16	−1.60
$RbBiInNbO_6$	1.29	4.30	2.97	6.30	−3.97	−1.73
$RbBiLuNbO_6$	1.22	4.14	1.76	5.38	−2.54	−1.86

Table 4. Rotation angle (in degrees) of the NbO_6 octahedron in various distorted phases of the compounds $Me^{+1}BiMe^{+3}NbO_6$ (z is the number of molecules in the unit cell)

Type of distortion	Symmetry group		Sc	Ga	In	Lu
φφφ	$R3(z=1)$	Na	6.0	6.2	6.9	7.1
		K	5.2	5.4	6.5	6.7
		Rb	5.2	5.5	6.1	6.7
φφψ	$Pc(z=2)$	Na	6.0	6.2	6.9	7.1
		K	5.2	5.4	6.5	6.7
		Rb	5.2	5.5	6.1	7.0
φφ0	$Cm(z=1)$	Na	7.3	7.3	8.2	8.4
		K	6.9	6.9	7.7	8.0
		Rb	6.5	6.5	6.1	7.9
0φψ	$C2(z=2)$	Na	7.3	7.3	8.4	8.6
		K	6.9	7.2	8.0	8.3
		Rb	6.5	6.8	7.7	8.3
φψψ	$P\text{–}4(z=4)$	Na	6.0	6.2	6.9	7.1
		K	5.2	5.9	6.5	6.7
		Rb	5.2	5.5	6.1	6.7

The dynamic charges of cations in the octahedron and of the component $O_{\|}$ are determined by the competition between the above contributions. In perovskite-like oxides, due to the high polarizability of the oxygen ion and due to the specific feature of the structure, the non-Lorentzian constants $\gamma_{ij}^{\alpha\beta}$ take large values in the directions of the Nb–O–Me^{3+} bond, which leads to the increase in the effective polarizability of the oxygen ion and, accordingly, to large values of dynamic charges. The short-range dipole–dipole interaction also contributes to the increase in dynamic charges. However, the short-range interactions between large dipoles and the spherically distributed charge density of the ions substantially reduce the Born charges (for example, numerical evaluations of various contributions to the dynamic charges for oxides with the elpasolite structure are presented in [6]).

In the compounds considered here, the dynamic charge of Me^{3+} depends both on the long-range and short-range interactions. On the one hand, the small values of the dipole polarizabilities of the Ga^{3+} (~0.1 Å^3) and Lu^{3+} (~0.06 Å^3) ions compared with the dipole polarizability of the Sc^{3+} and In^{3+} (~0.3 Å^3) ions substantially reduce the dipole–dipole contributions to the effective charge on the Ga^{3+} and Lu^{3+} ions compared with similar contributions on the Sc^{3+} and In^{3+} ions. Long-range dipole–dipole interactions also become weaker as the unit-cell parameter increases under the substitution Sc ⟶ Ga ⟶ In ⟶ Lu. On the other hand, short-range dipole–charge interactions between oxygen and a trivalent metal, which reduce the dynamic charge, increase with the number of Me^{3+} in the periodic table. For example, while, for identical values of the unit-cell parameters and the polarizabilities of the Sc^{3+} and In^{3+} ions, the dynamic charges (in the units of electron charge) on these ions with regard to all interactions amount to 5.2 and 2.3, respectively, for switched off short-range dipole–charge interaction of the pair O–Sc (In), these charges amount to 14.4 and 15.7, respectively.

3.2. Structure and Energy Characteristics of Distorted Phases

According to Table 2, the most unstable modes for all the compounds considered are threefold degenerate modes with eigenvectors (see Figs. 3a and 3b) corresponding to antiferrodistortive distortions denoted above by φ and ψ. The total energy of the crystal with 40-atom unit cell was minimized with respect to the amplitudes of displacements of oxygen ions for various combinations of φ and ψ distortions. Table 4 presents the displacements of oxygen ions (expressed in terms of the rotation angle of the NbO_6 octahedron) only for those combinations of φ and ψ distortions that lead to the lowest energy distorted phases. Table 4 shows that the distorted phases discussed here, except for the phase with distortion φψψ, are polar. A complete analysis of the symmetry of distorted phases for $Me^{I}Me^{II}Me^{III}Me^{IV}O_6$ compounds with cation ordering along the [111] direction of the perovskite structure was carried out in [7].

After the minimization of the crystal energy with respect to the combinations of φ and ψ distortions, we relaxed the structure, as described in Section 2, and calculated the lattice vibration frequencies in the relaxed structures. In the structures with distortions φφφ, φφψ, and 0φψ, all vibration modes turned out to be hard, while the polar structure φφ0 and the nonpolar structure φψψ retained the unstable polar modes. Therefore, to find a stable state for these structures, we minimized the total energy with respect to the amplitudes of displacements of ions with the eigenvector of this polar mode. The energies of the stable distorted phases obtained for the compounds are presented in Table 5. Note that the maximum contribution (of about 68–70%) to the difference between the energies of the cubic and distorted phases is made by the displacements of ions associated with the φ and (or) ψ distortions.

The polarization components per one structural unit of a crystal in stable polar phases are presented in Table 6, which shows that, for all the compounds, the most energetically favorable phase is a rhombohedral phase with one molecule in the unit cell and with polarization directed along the spatial diagonal of the original cubic phase. In this case, the polarization amounts to about 40 μC/cm^2. (Note that the polariza-

Table 5. Energy difference (in eV) between the cubic and distorted phases of the compounds $Me^{1+}BiMe^{3+}NbO_6$ (z is the number of molecules in the unit cell)

Type of distortion	Symmetry group		Sc	Ga	In	Lu
φφφ	$R3(z=1)$	Na	−0.405	−0.453	−0.760	−0.953
		K	−0.376	−0.411	−0.696	−0.858
		Rb	−0.377	−0.406	−0.683	−0.831
φφψ	$Pc(z=2)$	Na	−0.393	−0.448	−0.749	−0.950
		K	−0.334	−0.382	−0.665	−0.831
		Rb	−0.308	−0.354	−0.629	−0.776
φφ0 + Seg	$Cm(z=1)$	Na	−0.341	−0.399	−0.668	−0.840
		K	−0.303	−0.341	−0.604	−0.813
		Rb	−0.287	−0.304	−0.578	−0.721
0φψ	$C2(z=2)$	Na	−0.343	−0.396	−0.670	−0.843
		K	−0.291	−0.337	−0.601	−0.767
		Rb	−0.276	−0.312	−0.569	−0.722
φψψ + Seg	$P\bar{4}(z=4)$	Na	−0.320	−0.365	−0.617	−0.687
		K	−0.251	−0.297	−0.657	−0.677
		Rb	−0.327	−0.357	−0.484	−0.684

Table 6. Components of spontaneous polarization (in μC/cm^2) of the compounds $Me^{1+}BiMe^{3+}NbO_6$ in distorted phases (z is the number of molecules in the unit cell)

Type of distortion	Symmetry group		Sc			Ga			In			Lu		
			P_x	P_y	P_z	P_x	P_y	P_z	P_x	P_y	P_z	P_x	P_y	P_z
φφφ	$R3(z=1)$	Na	23	23	23	21	21	21	23	23	23	23	23	23
		K	24	24	24	22	22	22	24	24	24	24	24	24
		Rb	27	27	27	25	25	25	26	26	26	26	26	26
φφψ	$Pc(z=2)$	Na	8	8	0	5	5	3	6	6	4	15	0	0
		K	9	9	0	24	0	0	7	7	2	9	3	3
		Rb	11	11	0	8	8	0	9	9	0	6	6	3
φφ0 + Seg	$P1(z=1)$	Na	23	0	0	19	0	0	19	0	0	18	0	0
		K	24	0	0	23	3	0	23	0	0	23	0	0
		Rb	31	0	0	30	0	0	12	12	0	24	0	0
0φψ	$C2(z=2)$	Na	20	0	0	16	0	0	18	0	0	17	0	0
		K	22	0	0	17	0	0	19	0	0	18	0	0
		Rb	36	0	0	21	0	0	21	0	0	20	0	0
φψψ + Seg	$P2(z=4)$	Na	10	4	0	8	1	0	13	2	1	15	2	0
		K	9	9	0	9	8	0	8	8	0	8	7	0
		Rb	16	0	0	7	0	0	23	0	0	27	0	0

tion calculated here substantially differs from the polarization for scandium compounds calculated in [3], which amounts to about 70–80 μC/cm^2.) However, the energy of the polar monoclinic phase φφψ with two molecules per unit cell with in-plane polarization is very close to that of the rhombohedral phase, but the polarization in the former phase is substantially smaller than that in the rhomohedral phase (see Table 6). The other three polar phases (two monoclinic and one triclinic phases) are energetically less favorable, although in some compounds the difference between the energies of these phases and the energies of the φφφ and φφψ phases amounts to 300–500 K, and they can be implemented at high temperatures.

4. CONCLUSIONS

In concussion, we list the main results of this work.

Within a nonempirical ionic crystal model, we have calculated the lattice vibration spectra, the dielectric permittivity, the elasticity moduli, and the Born dynamic charges of the compounds $Me^{1+}Bi^{3+}Me^{3+}NbO_6$ (Me^{1+} = Na, K, Rb; Me^{3+} = Sc, Ga, In, Lu) in the cubic phase. There are two types of instabilities in all the compounds: antiferrodistorsive instability (threefold degenerate mode F_1 ($q = 0$) and a single mode X_2 $\left(q = \frac{2\pi}{a}(1, 0, 0)\right)$ and ferroelectric instability (threefold degenerate mode F_2 ($q = 0$)). The eigenvectors of these modes differ from the eigenvectors of the corresponding modes in perovskites and elpasolites.

We have established the symmetry of the five energetically most favorable distorted phases. Distortions with respect to the combinations of displacements of oxygen ions along the eigenvectors of the nonpolar modes F_1 ($q = 0$), X_2 $\left(q = \frac{2\pi}{a}(1, 0, 0)\right)$, and Y_2 $\left(q = \frac{2\pi}{a}(0, 1, 0)\right)$ followed by relaxation of the structures obtained as a result of displacements of oxygen ions yield, with one exception, polar phases. The spontaneous polarization in these phases is mainly associated with the displacements of Bi^{3+} ions from symmetric positions in the cubic phase. Thus, in four of the five low-energy phases discussed here, polarization of the crystal appears as a secondary effect (improper ferroelectricity).

A combination of oxygen ion displacements along one component of the mode F_1 and the modes X_2 and Y_2 leads to a nonpolar phase; however, the vibration spectrum of the lattice of all the compounds in this phase contains an unstable polar vibration mode. Further distortions of the structures along the eigenvector of this polar mode lead to a polar phase with stable lattice vibration frequencies. The ferroelectric instability also persists in a monoclinic polar phase obtained as a result of distortions of the cubic structure along two eigenvectors of the mode F_1. Further distortion of the structure of this phase along the eigenvector of the unstable polar mode again leads to a monoclinic phase with a different direction of the polarization vector.

The results of calculations of the structural and dynamic properties of the compounds $Me^{1+}Bi^{3+}Me^{3+}NbO_6$ in a cation-ordered phase, obtained in the present paper, show that the polar behavior of these compounds substantially differs from the behavior of the known simple and double oxides with perovskite structure; therefore, the experimental investigation of these properties of already synthesized compounds $NaBiScNbO_6$ and of as yet not synthesized compounds attracts interest.

ACKNOWLEDGMENTS

This work was supported by the Russian Foundation for Basic Research (project no. 09-02-00067) and by the program for the support of leading scientific schools (project no. NSh-4645.2010.2).

REFERENCES

1. K. M. Rabe, C. H. Ahn, and J.-M. Triscone, *Physics of Ferroelectrics: A Modern Perspective* (Springer, Berlin, 2007; Binom, Moscow, 2011).
2. Meghan Knapp, PhD Dissertation (Ohio State University, Columbus, Ohio, United States, 2006).
3. S. Takagi, A. Subedi, V. R. Cooper, and D. J. Singh, Phys. Rev. B: Condens. Matter **82**, 134108 (2010).
4. E. G. Maksimov, V. I. Zinenko, and N. G. Zamkova, Phys.—Usp. **47** (11), 1075 (2004).
5. O. E. Kvyatkovskii, Sov. Phys. Solid State **27** (9), 1603 (1985); O. Kvyatkovskii, Ferroelectrics **153**, 201 (1994).
6. V. I. Zinenko, N. G. Zamkova, E. G. Maksimov, and S. N. Sofronova, JETP **105** (3), 617 (2007).
7. N. Ter-Oganesyan, in *Abstracts of Papers of the 19th All-Russian Conference on Physics of Ferroelectrics, Moscow, June 20–23, 2011* (Moscow, 2011).

Translated by I. Nikitin